

Towards the atomistic simulation of phase coexistence in nonequilibrium systems

András Baranyai and Peter T. Cummings

Citation: *The Journal of Chemical Physics* **105**, 2378 (1996); doi: 10.1063/1.472105

View online: <http://dx.doi.org/10.1063/1.472105>

View Table of Contents: <http://scitation.aip.org/content/aip/journal/jcp/105/6?ver=pdfcov>

Published by the [AIP Publishing](#)

Articles you may be interested in

[Hydrodynamic boundary conditions for confined fluids via a nonequilibrium molecular dynamics simulation](#)
J. Chem. Phys. **105**, 3211 (1996); 10.1063/1.471836

[Simulating shear flow](#)
J. Chem. Phys. **104**, 5956 (1996); 10.1063/1.471327

[Multiple time step nonequilibrium molecular dynamics simulation of the rheological properties of liquid ndecane](#)
J. Chem. Phys. **104**, 255 (1996); 10.1063/1.470896

[Nonequilibrium molecular dynamics study of shear and shearfree flows in simple fluids](#)
J. Chem. Phys. **103**, 10217 (1995); 10.1063/1.469925

[Massively parallel computer simulation of planestrain elastic–plastic flow via nonequilibrium molecular dynamics and Lagrangian continuum mechanics](#)
Comput. Phys. **6**, 155 (1992); 10.1063/1.168448



Towards the atomistic simulation of phase coexistence in nonequilibrium systems

András Baranyai^{a)} and Peter T. Cummings

Department of Chemical Engineering, University of Tennessee, 419 Dougherty Engineering Building, Knoxville, Tennessee 37996-2200 and Chemical Technology Division, Oak Ridge National Laboratory, Oak Ridge, Tennessee 37831-6268

(Received 12 December 1995; accepted 29 April 1996)

A theoretical approach is presented which represents the first attempt known to the authors to develop molecular dynamics algorithms capable of modeling phase coexistence between two nonequilibrium steady state phases confined in a closed (E, V, N) system. We deal exclusively with shearing liquids because of their importance in rheology. In the present paper, as in the equilibrium Gibbs ensemble Monte Carlo technique for systems at equilibrium, the coexisting phases have no physical contact but their dynamics are coupled in order to reach mechanical, thermal, and composition balance between bulk regions of the two phases. The thermal balance is maintained by requiring zero net heat flow across a hypothetical boundary. This can be achieved by starting from equilibrium and gradually increasing the strength of the external field (the shear rate) in a quasistatic process. For particle interchanges we invoke the Evans–Baranyai variational principle which is at the very least a good approximation for similar simulated steady state systems far from equilibrium. Results of several model calculations are presented. The limitations and the implications of the methods are discussed. © 1996 American Institute of Physics. [S0021-9606(96)50630-6]

I. INTRODUCTION

Since the seminal work of Panagiotopoulos¹ numerous simulations have been performed in atomic/molecular detail to model liquid–vapor equilibrium. By providing a deeper understanding of phase separation and an important additional test for interaction potential models, it is not surprising that the so-called Gibbs ensemble Monte Carlo (GEMC) technique has become a commonly used computer simulation methodology.² Another important direction in computer simulation is represented by the nonequilibrium molecular dynamics (NEMD) methodology which mimics nonequilibrium steady state (NESS) systems far from equilibrium.³ The dynamics of these NESS systems are modeled in atomic/molecular detail just as in the case of equilibrium molecular dynamics (MD) simulations.⁴

The purpose of the present paper is to attempt to adapt the Gibbs ensemble technique to phase-coexistence problems in nonequilibrium systems. The best-known example of this phenomenon is the phase separation of polymer blends under the impact of shear.⁵ Our aim might seem straightforward: We have only to combine the Gibbs ensemble technique with a NEMD algorithm. Unfortunately, this is far from simple. Equilibrium methods such as the Gibbs ensemble simulation rely on the well-founded theory of equilibrium statistical thermodynamics, while the NEMD methods can utilize only linear response theory and the correctness of the dynamical picture depicted in the mechanical details of the simulation. There have been several attempts to extend the theory of linear irreversible thermodynamics to far-from-equilibrium situations.⁶ However, these attempts have been made on the

macroscopic, phenomenological level and provide only limited help in understanding these systems in the microscopic detail mandatory for developing simulation methodologies.

The lack of a well-established far-from-equilibrium thermodynamic theory is not a crucial problem if one is interested only in transport coefficients and structures of NEMD models. However, it is impossible to model the phase coexistence of NESS systems, without governing principles of general validity. The derivation of such general principles is fraught with difficulty. Even the definition of the state of a NESS system is a nontrivial matter. As a result of several NEMD studies and theoretical considerations, it seems reasonable to believe that the concept of temperature acquires different attributes in far-from-equilibrium situations.^{6–10}

Despite all the difficulties, we believe that the theoretical framework proposed in this paper can serve as the starting point for further efforts in this direction. We discuss possible approaches and their limitations in terms of their theoretical correctness and numerical feasibility. Since NEMD algorithms cannot be formulated in a stochastic manner, we first present the derivation of our equilibrium molecular dynamics version (GEMD) of the GEMC simulation for a total system represented by the microcanonical (E, V, N) ensemble. The algorithm for the usual canonical (T, V, N) ensemble has already been given elsewhere.¹¹ A similar derivation was obtained recently by Palmer and Lo¹² but their equations of motion are more complex than ours. Our approach yields a simpler algorithm which can be implemented with minor modifications of a standard molecular dynamics code.

In Sec. III we extend our algorithm to a system consisting of two phases under the impact of an external field. The most important practical case is when the external field is the strain rate or strain stress of shear flow. Fortunately, the NEMD algorithm for this problem, the so-called SLLOD al-

^{a)}Permanent address: Eötvös University, Laboratory of Theoretical Chemistry, Budapest 112, P.O. Box 32, 1518, Hungary.

gorithm is considered to be exact even outside of the linear regime.³ The SLLOD algorithm can be used to model planar Couette flow of liquids simulated at the atomic/molecular level.

An indispensable part of every NEMD algorithm is the synthetic thermostat (or ergostat), which is a microscopically reversible feedback scheme controlling the temperature (or the energy) of the system. Without a synthetic thermostat the system becomes inhomogeneous and consequently ill-defined. By the term “synthetic” we mean the now-common approach in MD simulations when the Hamiltonian equations of motion are supplemented with a linear friction term, $-\alpha \mathbf{p}$ which can be derived from Gauss’s principle of least constraint.³ The thermostating multiplier, α can be determined either from a differential feedback (the Gaussian case) or from an integral feedback (the Nosé–Hoover case).³ In equilibrium for ergodic systems both of these cases describe a dynamics which selects the states from well-defined statistical mechanical ensembles, the isokinetic and the canonical ensembles, respectively. For systems far from equilibrium (beyond the linear regime) there is no rigorous theoretical justification for these schemes other than the equilibrium analogy. Nevertheless, simulations and theoretical studies have demonstrated that this linear form is not only simple but consistent with the principles applied in the further part of our present paper.^{13,14}

Since the condition of mechanical stability is relatively straightforward even in NEMD calculations, the crucial problem is to model the heat balance between the coexisting phases correctly. We wish to achieve this, as in the Gibbs ensemble simulation technique, without creating a real interface between the two phases. The presence of a real interface considerably distorts the modeled macroscopic properties unless the bulk regions are much bigger than the interface region. In addition to this, our experience indicates that at high shear rates where the structure of the shearing liquid is considerably different from that of the equilibrium liquid, the penetrability of the interface is much smaller than in equilibrium. As in the case of the high-shear-rate string phase, the system can stay in a metastable state for a long time.¹⁵ A discussion of these problems in NEMD simulations is an essential part of Sec. III.

The ultimate thermodynamic basis of the calculations is the variational principle of Evans and Baranyai (EB).¹⁶ This principle was proposed as a nonlinear generalization of the minimum entropy principle.¹⁷ Although the exactness of the EB principle in the nonlinear regime is in doubt,^{14,18,19} computer simulation results have shown that it is at least an excellent approximation.^{20–22} Besides its numerical feasibility, the EB principle is closely related to a well-known, macroscopic entropy definition.²³ This supports the application of this principle proposed originally as a *local* extremum property to *global* balance problems such as phase separation. We will discuss the implications of this principle at length in Sec. III.

In Sec. IV, we present results of approximate phase-coexistence simulations for a particular shearing system. The purpose of this calculation was to find a simple model mix-

ture which exhibits a strong tendency to separate under the impact of shear. Identifying a model system that can be used to test algorithms for phase equilibrium in systems under shear is an important element in ultimately verifying the accuracy and efficiency of such algorithms. We find that the model system we propose is only marginally useful in this context. Finally, Sec. V contains our conclusions.

The philosophy of this paper can be summarized as follows: Our goal in this work is to focus attention on the problem of predicting phase equilibria in nonequilibrium systems, and to make a tentative first step towards developing an algorithm for the efficient simulation of phase equilibrium in such systems. Before one can develop such an algorithm, the conditions for phase equilibrium in a NESS system must be established. Thus our paper consists of three elements: conjecture on the appropriate conditions for phase equilibria in NESS systems; translation of those conditions into an algorithm (in which we are forced to introduce approximations since we were unable to derive exact algorithmic implementations of all the conjectured conditions for phase equilibrium); and application of the approximate algorithm to a system which has the potential to exhibit phase equilibrium under shear. In all three elements, we present initial steps in directions that we hope will ultimately lead to a rigorous, efficient algorithm for phase equilibrium in NESS systems that can be applied to systems of practical interest, i.e., polymer blends subjected to shear.

II. MOLECULAR DYNAMICS ALGORITHM OF PHASE EQUILIBRIUM SIMULATION

According to the Gibbs ensemble method of Panagiotopoulos^{1,24} the bulk properties of coexisting phases can be studied with no physical contact and no interface between the two regions. The states of the two subsystems, one for each phase, are sampled by applying the usual Markov chain technique of Monte Carlo simulations. The acceptance criteria are formulated to fulfill thermodynamic equilibrium between the two phases under the condition that the two phases together form a system which is representative of the canonical ensemble at constant total volume, V , total number of particles, N , and temperature, T . Random displacements, volume rearrangements, and particle interchange steps are performed to achieve mechanical and chemical equilibrium between the two phases. The extension of the method to multicomponent systems is straightforward. The MD version of the GEMC method has been derived recently¹² where the same approach was translated into the deterministic language of extended Hamiltonians.

Unlike the GEMC method our system is closed, representing a member of a microcanonical ensemble at fixed total internal energy, E , instead of the uniform temperature, T . This is different from the standard canonical version of the GEMD algorithm which was presented in our previous paper.¹¹ The choice of the seemingly unusual microcanonical condition is motivated by the requirements of nonequilibrium simulations. The internal energy, E , is a much more well-defined state variable for NESS systems than the am-

biguous temperature. This feature of the derivation will be exploited later for NESS systems.

The two simulation cells, each chosen from regions deep inside phase 1 and phase 2 are characterized by the following constraints:

$$V = V_1 + V_2, \quad E = E_1 + E_2, \quad (1)$$

$$N = N_A + N_B, \quad N_A = N_{A1} + N_{A2}, \quad N_B = N_{B1} + N_{B2},$$

where the subscript indices refer to the corresponding phases. For the sake of simplicity we have only two chemically different components (*A* and *B*) in the system. The conditions of equilibrium between the two phases can be expressed by the equivalence of the intensive parameters conjugate to the extensive state variables of Eq. (1)

$$P_1 = P_2, \quad T_1 = T_2, \quad \mu_{A1} = \mu_{A2}, \quad \mu_{B1} = \mu_{B2}. \quad (2)$$

In the following we derive equations of motion that strictly maintain the constraints of Eq. (1) while guiding the composite system towards the mechanical, thermal, and chemical equilibrium conditions of Eq. (2). We start from the equations of motion written in the more convenient Hoover form²⁵

$$\dot{\mathbf{q}}_i = \frac{\mathbf{p}_i}{m_i} + \epsilon(\mathbf{q}_i - \mathbf{R}_0),$$

$$\dot{\mathbf{p}}_i = \mathbf{F}_i - \epsilon \mathbf{p}_i - \alpha \mathbf{p}_i, \quad (3)$$

where \mathbf{q}_i , \mathbf{p}_i , are the position and momentum of particle *i*. The force acting on this particle is \mathbf{F}_i , its mass is m_i , and \mathbf{R}_0 is the center of mass of the system. The variable ϵ acts as a strain rate factor coupling the system to a barostat and α is the feedback multiplier coupling the system to a heat bath. These equations govern the dynamics of both regions (1 and 2) in our closed system. However, there is an important difference between this approach and the usual MD simulations with thermodynamic constraints when the barostats and thermostats are coupled to infinitely large reservoirs. Our two phases are of comparable size so fluctuations in the pressure of system 1, for instance, will have an impact on the dynamics of system 2. Thus, the two phases evolve simultaneously towards equilibrium.

A. Mechanical equilibrium

Using ϵ we can express the change in the volume

$$\dot{V}_j = 3V_j\epsilon_j, \quad \text{or} \quad \dot{L}_j = L_j\epsilon_j, \quad (4)$$

where L_j is the length of cubic box *j*, $j=1,2$. In order to obtain equations for $d\epsilon_j/dt$ while maintaining the restriction of constant volume we have to differentiate the first condition of Eq. (1) twice with respect to time,

$$V_1(3\epsilon_1^2 + \dot{\epsilon}_1) + V_2(3\epsilon_2^2 + \dot{\epsilon}_2) = 0. \quad (5)$$

We now have several options for relating $d\epsilon_j/dt$ to the pressures of the two phases. The following expression seems to be the best candidate for this purpose:

$$\dot{\epsilon}_1 = \frac{1}{V_1 W} (P_1 - P_2) - \frac{3}{2} (\epsilon_1^2 + \epsilon_2^2 V_2/V_1)$$

$$(6)$$

$$\dot{\epsilon}_2 = \frac{1}{V_2 W} (P_2 - P_1) - \frac{3}{2} (\epsilon_2^2 + \epsilon_1^2 V_1/V_2),$$

where W is a constant. According to Eq. (6) the relative volume changes are determined entirely by the difference in the instantaneous pressures.¹¹ This becomes obvious if one examines the following difference:

$$V_1 \dot{\epsilon}_1 - V_2 \dot{\epsilon}_2 = \frac{2}{W} (P_1 - P_2). \quad (7)$$

B. Thermal equilibrium

The internal energy of system *j* is defined as follows:

$$E_j \equiv \sum_{i=1}^{N_j} \frac{\mathbf{p}_{ij}^2}{2m_i} + \Phi(\mathbf{q}_j^N), \quad (8)$$

where the second term on the right-hand side of Eq. (8) represents the configurational energy. The change of the internal energy of system *j* with respect to time from Eqs. (3) and (8) is given as

$$\dot{E}_j = -(p_{xx} + p_{yy} + p_{zz})_j V_j \epsilon_j - \alpha_j K_j, \quad (9)$$

where the first term represents the work of the pressure, (p_{xx} , p_{yy} , and p_{zz} are the corresponding diagonal elements of the pressure tensor) and the second term represents the heat pumped in or out of the system

$$\left(K_j \equiv \sum_{i=1}^{N_j} \frac{\mathbf{p}_{ij}^2}{m_i} = 3N_j k T_j \right).$$

In this definition T_j is the *kinetic* or *equipartition* temperature of phase *j* which is identical to the thermodynamic temperature of the same phase only in equilibrium.⁶⁻¹⁰ To keep the internal energy of the combined system fixed we require the following equation to hold:

$$\dot{E}_1 + \dot{E}_2 = 0. \quad (10)$$

Besides Eq. (10) we want thermal equilibrium between the two systems. If we choose identical starting temperatures [$T_1(0) = T_2(0)$] then by maintaining at every time step the following condition

$$\frac{dT_1}{dt} = \frac{dT_2}{dt}, \quad (11)$$

we ensure that during the course of the simulation the two systems will have identical random kinetic energies, i.e., temperatures. From Eqs. (3), (11), and the definition of K_j we get

$$\frac{dT_j}{dt} = \frac{2}{3N_j k} \sum_{i=1}^{N_j} \mathbf{p}_{ij} \dot{\mathbf{p}}_{ij} / m_i$$

$$= \frac{2}{3N_j k} \left(\sum_{i=1}^{N_j} \mathbf{F}_{ij} \mathbf{p}_{ij} / m_i - \epsilon_j K_j - \alpha_j K_j \right). \quad (12)$$

Now, using Eqs. (9)–(12) we can determine the thermostatting multipliers, α_1 and α_2 ,

$$\begin{aligned} & \left(1 + \frac{N_2}{N_1}\right) K_1 \alpha_1 \\ &= -3(\epsilon_1 p_1 V_1 + \epsilon_2 p_2 V_2) + \frac{N_2}{N_1} \sum_{i=1}^{N_1} \mathbf{F}_{i1} \mathbf{p}_{i1} / m_i \\ & \quad - \sum_{j=1}^{N_2} \mathbf{F}_{j2} \mathbf{p}_{j2} / m_j + \epsilon_2 K_2 - \frac{N_2}{N_1} \epsilon_1 K_1, \end{aligned} \quad (13)$$

where the hydrostatic pressure is, $p = (p_{xx} + p_{yy} + p_{zz})/3$. The equation for α_2 is formally the same and is obtained by reversing the indices 1 and 2 in Eq. (13). In this formulation the pressure balance is given in the form of an integral feedback while the thermal equilibrium is given by a differential feedback. As expected, the total volume will be preserved much more accurately than the total energy because the former is constrained at the level of second derivatives. One could derive equations in which both conditions are expressed in the form of an integral feedback. In order to do so, one must take the time derivative of Eqs. (9) and (10) then express $d\alpha/dt$ in a similar fashion as $d\epsilon/dt$ is given in Eq. (6). This approach, however, is less convenient because the time derivatives of the pressure contain derivatives of the interparticle forces.

C. Composition equilibrium

Entropic quantities are functionals and not phase variables of the system. Thus, in the size ranges of computer simulations their estimates always require long-run averages or integrations. This means that, unlike in the case of the pressure or the temperature one cannot devise a simple and workable feedback scheme for maintaining identical chemical potentials in the two phases. Assuming the ergodicity of the dynamical system, however, one can incorporate particle interchanges into the algorithm in a stochastic manner.¹¹

We assume that the probability of the interchange step is unchanged from the usual Gibbs ensemble formula given by

$$P = \exp\left(-(\Delta U_1 + \Delta U_2)/kT(t) - \ln \frac{V_2(N_1 + 1)}{V_1 N_2}\right), \quad (14)$$

where ΔU_1 is the energy difference in subsystem 1 caused by particle creation and ΔU_2 is the energy difference in subsystem 2 caused by particle removal, $T(t)$ is the actual temperature, identical in the two subsystems. Equation (14) is justified because at the stochastic interchange step the dynamics stops and this snapshot of our system is identical with that of a canonical composite system at a fixed temperature, $T(t)$.

Since our composite system is modeled in the microcanonical ensemble (E, V, N) the algorithm is different from the standard constant temperature case.²⁴ The total energy of the particle removed from phase 1 should be identical to the total energy of the particle inserted into phase 2. To achieve this the random kinetic energy of the inserted particle is determined by the energy difference between the total energy of the removed and the configurational energy of the inserted particle. This will slightly offset the rigorous equivalence of

the temperatures in the two phases because the new kinetic energy in both subsystems will be different from the old one. This inconsistency is the result of the differential temperature control. We could avoid this problem by invoking integral feedback for the energy constraint but the price—as we alluded to earlier—is too high: it requires the calculation of the derivatives of the forces. Instead of that, after the particle exchange we rescale the velocities in both systems to have identical temperatures and fixed total energy. The resulting velocity changes are negligible.

The above algorithm is hybrid in a sense that deterministic and probabilistic elements are combined. We have to halt our MD run after n time steps to perform the particle interchange steps. (In principle we should use a self-starting integrator after each particle interchange but this would increase the cost of the calculation and complicate the program code, so we neglect the small errors introduced by the inaccurate first time-step integrations.)

D. Long-range correction

There is a very important technical problem in computer simulations which has not been addressed thus far in this paper. Since we omit the explicit calculations of particle interactions beyond a certain separation (the so-called cutoff distance), we have to correct our results to compensate for the missing long-range part of the potential. Both the internal energy and the pressure have long-range contributions. These contributions are calculated using the assumption that beyond the cutoff the pair-correlation function is unity.⁴ Since the densities of the coexisting phases might be different the long-range corrections have to be included in the formulation of the equations. In the case of the pressure we have already distinguished the corrected or full pressure using uppercase P from the uncorrected pressure obtained in Eq. (9) using lowercase p . It is important to note that while in Eqs. (6) and (7) the pressure must be corrected, in equations dealing with energy conservation this must not be done since errors in the energy are corrected separately. In the case of Lennard-Jones particles the energy correction can be given in analytic form:⁴

$$E_{\text{LJcorr}} = \frac{8\pi N^2}{V} \left(\frac{1}{9r_c^9} - \frac{1}{3r_c^3} \right) = C \frac{N^2}{V}, \quad (15)$$

where C is a constant during the course of the simulation. This term should be added to the energy of Eq. (8) calculated within the cutoff distance, r_c . The change in the energy correction comes merely from the change in the volumes,

$$\dot{E}_{\text{Jcorr}} = - \frac{3CN_j^2 \epsilon_j}{V_j}. \quad (16)$$

Equation (15) must be added to Eq. (9) and the further derivation should be performed accordingly.

III. ALGORITHM FOR SIMULATING PHASE COEXISTENCE IN NONEQUILIBRIUM STEADY STATES

We follow the same approach as in Sec. II. The NESS system to be modeled consists of two regions, each chosen from the bulk part of the corresponding phase. In this paper we will not deal with questions related to the common phase boundary of the coexisting phases. Constant pressure SLLD equations of motion simulating planar Couette flow can be given analogously to Eq. (3),

$$\begin{aligned}\dot{\mathbf{q}}_i &= \frac{\mathbf{p}_i}{m} + \epsilon(\mathbf{q}_i - \mathbf{R}_0) + \mathbf{i}\gamma y_i, \\ \dot{\mathbf{p}}_i &= \mathbf{F}_i - \epsilon\mathbf{p}_i - \mathbf{i}\gamma p_{yi} - \alpha\mathbf{p}_i,\end{aligned}\quad (17)$$

where $\gamma \equiv \partial u_x / \partial y$ is the shear rate and \mathbf{i} is the unit vector in the x direction. The momenta are peculiar, i.e., they are measured relative to the local streaming velocities.

In the case of NESS systems the constant E , V , N conditions are the only well-defined macroscopic constraints due to the uncertainty of the concepts of thermodynamic temperature and pressure. Thus, we will keep these state variables constant while seeking mechanical, thermal, and compositional balance.

A. Mechanical balance

Our first consideration is the possible relationship between the mechanical definition of the pressure (the pressure tensor) and the thermodynamic definition of the pressure. It has been suggested based on computer experiments⁶ and theoretical considerations²⁶ that the thermodynamic pressure corresponds to the minimal eigenvalue of the pressure tensor. This conjecture seems plausible if one thinks about the pressure in terms of the minimum amount of work necessary to change the volume of the NESS system. Obviously, this choice could be easily incorporated into the algorithm by replacing the hydrostatic pressure with the minimum eigenvalue of the pressure tensor. This conjecture, however, is not yet proven. An important usage of this algorithm could be to provide further numerical evidence which can verify or refute this conjecture.

A more obvious requirement of mechanical equilibrium is that diagonal components of pressure tensors perpendicular to the plane of the common phase boundary must be equal. If the normal vector of the phase boundary between the two phases is parallel with the y axis then P_{yy} should be written in Eq. (6) instead of P . We can also decouple the different directions of our simulation box and allow changes in box lengths only in directions perpendicular to the phase boundary. No matter what the proper definition of the thermodynamic pressure is this trivial equilibrium should hold between two steady state systems. We believe that in coexisting NESS systems the steady phase boundary (maintained by the equal pressures of the two phases) automatically ensures the equality of the thermodynamic pressure. This provides two constraints between the four independent elements of the two pressure tensors.

B. Thermal balance

Although there is uncertainty about the proper definition of the thermodynamic pressure, one continues to use the same equations (i.e., equality of the pressures in the two phases) used at equilibrium. In the case of the thermal balance, however, we have to generalize the equality of temperature conditions used at equilibrium. If we imagine two macroscopic phases under the impact of the same dissipative field, the heating up of the two regions will be different in general. The change in the temperature locally is determined by the ratio of the rate of heat dissipation and the specific heat of the phase. Since these ratios are not equal for the two phases, heat will flow from the warmer phase to the colder one. We require zero net heat flow across the boundary between phases 1 and 2 as an operational definition of thermal balance. In addition to this, as in the single phase NEMD algorithms we want homogeneous phases without temperature gradients within. (This is in contrast with the ‘naive’ or ‘brute force’ approach where the phase separation simulation is performed in a single but very large simulation cell. Since the system size is still far from macroscopic the simultaneous presence of a strong heat flow could introduce large inhomogeneities.)

The change in the energy with time is the rate at which heat is produced minus the energy removed from the system by the synthetic thermostat. For phase j ,

$$\dot{E}_j = -3p_j\epsilon_j V_j - p_{xyj}V_j\gamma - \alpha_j K_j \equiv \dot{Q}_j - \alpha_j K_j, \quad (18)$$

where dQ_j/dt is the rate of heat produced in phase j . Equation (18) differs from Eq. (9) only by the presence of the viscous heat. We have to determine the two α 's for the two phases maintaining the condition of Eq. (10). The first equation is simply the formulation of this requirement,

$$\begin{aligned}\alpha_1 K_1 + \alpha_2 K_2 &= -3p_1 V_1 \epsilon_1 - 3p_2 V_2 \epsilon_2 - p_{xy1} V_1 \gamma \\ &\quad - p_{xy2} V_2 \gamma.\end{aligned}\quad (19)$$

The thermostats of the two subsystems should remove the energy increase of the composite system. Equation (19), however, makes no assumption about how the energy should be redistributed between the two subsystems. To achieve thermal balance we introduce a thermodynamic temperature, T_{th} . We do not investigate the relation of this quantity to any other previously introduced nonequilibrium temperature concept. For our present purposes this is simply the variable which governs the heat flow between the two phases. If the thermodynamic temperatures of the two phases are equal then the net heat flow through the hypothetical phase boundary should be zero. We know no way to determine this quantity *a priori*. Obviously, the accurate value of the thermodynamic temperature is a complicated function of the other state variables. We can, however, avoid this difficulty by using only the time derivative of the thermodynamic temperature. The same approach was used in the equilibrium case in Eq. (11). The following equality

$$\dot{T}_{th1} = \dot{T}_{th2} \quad (20)$$

ensures that the thermal balance will be preserved provided at $t=0$ the two temperatures were equal. There is only one state of our system where we can easily establish this thermal balance: the equilibrium state. (This already indicates that the entire model calculation should start from the equilibrium state of the same system.)

The change in the thermodynamic temperature can be expressed as the ratio of the heat production and the heat capacity of that phase,

$$\dot{Q}_1/c_{\text{th}1} = \dot{Q}_2/c_{\text{th}2}. \quad (21)$$

The thermodynamic heat capacity is also a difficult property to determine. Fortunately, we can replace it with the kinetic heat capacity. The kinetic heat capacity is the derivative of the heat by the kinetic or equipartition temperature of the system,

$$c_{\text{th}} = \frac{dQ}{dT_{\text{th}}} = \frac{dQ}{dT_K} \frac{dT_K}{dT_{\text{th}}} = c_K \frac{dT_K}{dT_{\text{th}}}. \quad (22)$$

From Eqs. (21) and (22) we obtain

$$\frac{\dot{Q}_1}{c_{K1}} \frac{dT_{\text{th}1}}{dT_{K1}} = \frac{\dot{Q}_2}{c_{K2}} \frac{dT_{\text{th}2}}{dT_{K1}}. \quad (23)$$

We can rewrite Eq. (23) as

$$\frac{\dot{Q}_1}{c_{K1}} \frac{dT_{\text{th}1}}{dt} \frac{dt}{dT_{K1}} = \frac{\dot{Q}_2}{c_{K2}} \frac{dT_{\text{th}2}}{dt} \frac{dt}{dT_{K2}}. \quad (24)$$

Using Eq. (20) we can eliminate the thermodynamic temperature

$$\dot{T}_{K1} \frac{c_{K1}}{\dot{Q}_1} = \dot{T}_{K2} \frac{c_{K2}}{\dot{Q}_2}. \quad (25)$$

The time derivative of the kinetic temperature can be expressed from the equations of motion using the definition of the kinetic temperature. In the case of phase j

$$\begin{aligned} \dot{T}_{Kj} &= \frac{2}{3N_{jk}} \sum_{i=1}^{N_j} \mathbf{p}_{ij} \dot{\mathbf{p}}_{ij} / m_i \\ &= \frac{2}{3N_{jk}} \sum_{i=1}^{N_j} \mathbf{p}_{ij} (\mathbf{F}_{ij} - \mathbf{i} \gamma p_{yij} - \epsilon_j \mathbf{p}_{ij} - \alpha_j \mathbf{p}_{ij}). \end{aligned} \quad (26)$$

The combination of Eqs. (25) and (26) gives the second equation [completely analogous to Eq. (13)] which is necessary to determine the two thermostating multipliers. Two things are mandatory for this scheme to work. First, in the initial state the two temperatures have to be equal. This means that the simulation has to start from equilibrium where the temperatures of the two phases are identical as we alluded to above. Second, we have to know the kinetic heat capacities of the two phases at every instant of the simulations.

Since the heat capacities of the NESS system are unknown we have to determine them during the transition. There are formulas in the literature for the kinetic heat capacity of NESS systems.³ They have been derived (in the $t \rightarrow \infty$ limit) after $t=0$ a constant external field was turned on.

Our previous manipulations, however, might lose their validity due to the singularity of system properties at $t=0$. Thus, we have to choose a direct method instead which calculates the kinetic heat capacity using numerical derivation. The most straightforward way to do this is to attach to both phases an auxiliary system. The auxiliary system of phase 1 will interact with the auxiliary system of phase 2. The two auxiliary systems form a composite system with the same total volume, number of particles but with slightly higher energy than the original system. The energy of the auxiliary phases is coupled to maintain equivalent temperatures but the changes in their volumes strictly follow the changes of their master systems. The latter property is necessary because during the simulation neither the pressures nor the volumes of the two systems are constant. The kinetic heat capacities of Eq. (25) are still well-defined because the auxiliary system makes identical volume fluctuations as the real one. (In fact, even if one performs phase coexistence simulations in a closed equilibrium system, the heat capacities of the two phases have to be taken into account otherwise the fluctuations of the two phases will be incorrect.)

The energy difference between the original and the corresponding auxiliary phase divided by their temperature difference estimates the kinetic heat capacity.

C. Composition balance

In the case of the mechanical balance the equilibrium expressions could be retained, while for thermal balance we still could devise an algorithm which is able to redistribute the thermal energy between the two phases correctly without modeling real heat flow. As a matter of fact, we did not make any approximations or particular assumptions about the nature of the thermodynamic temperature other than it is a continuous, differentiable function of the kinetic temperature. The difficulties of the composition balance formulation however, are more severe. One has to define a generalized chemical potential if one wants to preserve the analogy with the equilibrium case.

There is a very widely used method in computer simulations to determine the chemical potential in equilibrium liquids. The so-called test particle or Widom method²⁷ can easily be derived from the canonical partition function.²⁸ The excess chemical potential is given as follows:

$$\beta \mu^{\text{ex}} = -\ln \langle \exp(-\beta \varphi) \rangle, \quad (27)$$

where $\beta=1/kT$ and φ is the energy change caused by the insertion of the test particle. If the particles interact as hard spheres the Boltzmann factor can have only two different values: 1 if the test particle overlaps with any other particle in the system, and 0 if it does not overlap.

1. Approximately modeled composition balance

There is no counterpart of the Gibbsian ensemble theory for NESS systems. We do not know what is the form of the time-independent Boltzmann factor under these circumstances. Nevertheless, the descriptiveness of the Widom method suggests that a similar approach is not entirely meaningless in NESS systems. Recently, Borzsák and Baranyai²⁹

used this method to estimate an upper bound for a generalized NESS chemical potential. They studied a shearing, two-dimensional SLLOD fluid with approximated hard core interaction. (Approximation was necessary because to devise a NEMD algorithm for hard particles is very difficult due to the nonlinear trajectories caused by the continuously acting external field and thermostat.) An advantage of the hard core interaction is that whatever is the form of the NESS Boltzmann factor the equilibrium scheme prevails. If the test particle overlaps with a real particle the insertion attempt is rejected. Otherwise the test particle “does not feel” the presence of the other particles, thus the probability of the insertion for such cases is 1.

Since the local structure of the shearing liquid is different from that of the equilibrium liquid the corresponding inserting probabilities will also differ. The test particle method assumes that there are no velocity–velocity or velocity–position correlations. There is evidence from computer experiments, however, that the random velocities superimposed on the streaming velocities are no longer Maxwell–Boltzmann in character in strongly shearing liquids.³⁰ As the shear rate increases the velocity distribution becomes more and more distorted and correlated with particle positions.³⁰ Thus, the calculated insertion probabilities give a measure of the distortion of the configurational phase space of the system by shear flow but tell us little about the entire (momentum and position) phase space volume. So the application of the Widom method is only an approximation even for hard particles where the problem of the proper definition of the Boltzmann factor (and the temperature in it) can be avoided.

It seems probable, however, that contributions from the velocity–velocity and velocity–position correlations are much smaller than the changes in position–position correlations which justify the usage of this approximation. In addition to this if the local, shearing dynamics is not very different in the two phases the error introduced by this simplified particle exchange step might largely cancel out.

2. Composition balance based on the EB principle

A few years ago Evans and Baranyai¹⁶ conjectured a variational principle for ergodic, NESS systems far from equilibrium. This principle states that if the internal energy, E , the volume, V , the number of particles, N and the external field, F_e is kept constant the absolute rate of compression of the phase-space volume which is accessible to the system is a local minimum with respect to variations in internal parameters of the system. This principle is a nonlinear generalization of the minimum entropy production principle which is valid only close to equilibrium where both the local thermodynamic equilibrium assumption and the Onsager reciprocal relations are expected to hold.¹⁷ Evans and Baranyai could not prove their hypothesis but provided simulation data supporting the conjecture.

So far all numerical studies carried out using NEMD simulations have confirmed this behavior.^{20–22} However, it has been shown recently by Santos *et al.*^{14,18,19} that an exact

solution of the nonlinear Boltzmann equation does not verify the principle. They found that the EB principle is only exact to first order in the shear rate, i.e., it does not go beyond the range of the minimum entropy production principle. Since the techniques applied in their study are exact in the sense of kinetic theory, this implies that the EB principle is only a good approximation beyond the linear regime. However, the thermostats of the theoretical model of Ref. 18 and of the simulated system differ: The EB principle was found in a generalized microcanonical ensemble (E, V, N, F_e) where an ergostat maintained the prescribed steady state, while Santos *et al.*¹⁸ used a *constant* thermostat variable. The significance of this difference is still unclear.

Nevertheless, there is no other easily applicable theory which could be used as an extremum principle for our present purpose. A further advantage of the EB principle is that the phase space compression factor is a simple phase variable which can easily be calculated in computer simulations. It is trivially related to the thermostating multiplier, α ,

$$\frac{d \ln f(\Gamma, t)}{dt} = - \frac{\partial}{\partial \Gamma} \dot{\Gamma} \equiv \Lambda(\Gamma, t) = -3N\alpha(\Gamma, t) + O(1), \quad (28)$$

where $f(\Gamma, t)$ is the phase space distribution function at time t and point Γ . The phase space compression factor, $\Lambda(\Gamma, t)$ due to this definition is always negative for dissipative systems. Order 1 differences are marked by the symbol of $O(1)$. It is the *mean value* of the phase space compression factor, $\langle \Lambda(\Gamma, t) \rangle$ which is a local maximum with respect to variations of internal parameters of the system. (This is simply the manifestation of the fact that the phase space compression factor is a phase variable and not a functional, therefore it should be averaged for all the possible microstates of the system.) Since the fluctuations in the phase space compression factor are considerably larger than the differences of its mean value for nearby steady states, one needs to perform long calculations to sense these differences accurately.

The minimum entropy production principle is a *local* extremum principle. It seems plausible to assume that its microscopic, generalized version (whether it is exact or just approximate far from equilibrium) is a local principle too. Thus, it cannot be applied to phase transitions which require a potential having *global* extremum property.

Recently, Baranyai²³ has shown that the EB principle is related to a well-known macroscopic nonequilibrium entropy definition.⁸ In this definition the minimum excess work performed on the system during the transition from its equilibrium state to a NESS defines the entropy difference between these two states. The minimum excess work is that small part of the entire work which does not dissipate during the quasistatic transition. The idea behind the approach is the equilibrium analogy. Keeping the internal energy fixed one can measure the entropy change by the quasistatic compression of the system using the second postulate of equilibrium thermodynamics.³¹ In the nonequilibrium computer experiment it was the shear rate which performed work on the system by bringing it infinitely slowly from equilibrium to a

well-defined NESS.⁸ The details of the above computer experiment as a realization of an old NESS entropy definition are important because the connection to the EB variational principle was made for this particular thought experiment. This derivation makes it possible to consider the EB principle as a microscopic manifestation of a macroscopic extremum property. The maximum of the NESS entropy relative to nearby states of the system furnishes us with the necessary governing criterion for phase-coexistence problems provided we perform the computer experiment analogously.

It is not surprising that this NESS entropy definition is connected to the equilibrium state of the system with the same (E, V, N) values just as in the case of the thermal equilibrium algorithm derived in Sec. III C 1. Equilibrium thermodynamics serves as a well-defined base from which we can reach out to as-yet-unknown territories of nonequilibrium theories.

The exploitation of the EB principle for particle interchange is more laborious than the equilibrium scheme. We have a two-phase two-component system. There are four possible interchange possibilities unless at least one of the phases contains only one type of particles. The ease or difficulty of the insertion attempt does not define the acceptance as in equilibrium, although as an approximate preselection it might indicate the final outcome. The ultimate criterion is given by $\langle \Lambda \rangle$. Before inserting and deleting a particle we have to store the entire information necessary to restart the program from the same phase space point. After interchange we follow the new trajectory for a long time calculating the average of the compression factor. Then we compare the new $\langle \Lambda \rangle$ with the old one. If it is larger (note that $\langle \Lambda \rangle$ is a negative quantity) we attempt to make the same type of interchange again. If it is smaller we try the other possible interchanges. If none of the interchanges is possible we increment the external field by a small amount and continue the simulation at this higher shear rate.

It is obvious that the EB principle could be used as a criterion for the heat balance as well. In this case, however, the number of trial procedures would be doubled because in addition to particle interchanges one had to increase or decrease the temperature too. The kinetic temperatures of the two phases should not be equal, so the exploration should allow for this possibility while maintaining the energy of the composite system at its fixed value.

A very important rule of the whole procedure is that the system must not be very far from its maximum entropy state because the validity of the EB principle is linked to this condition. So the particle interchanges cannot involve more than one particle at a time while the temperature changes should be performed by a sufficiently small increment. It is a weakness of this approach that if one gets too far from the maximum entropy path all the following states of the system might be erroneous. Unfortunately, there is no criterion which would indicate the derailing of the transition process.

IV. APPLICATION TO SIMPLE MODEL MIXTURES

The proposed algorithm should ideally be tested on a model which is known to exhibit a high degree of strain rate dependence in its phase equilibria. Experimentally, such systems are typically polymer blends that demix under the action of shear. Atomistically detailed simulation of such models is prohibitively expensive and beyond our computing capabilities at this time. With the goal of identifying a simple, computationally inexpensive model fluid which exhibited phase separation under the action of shear, we investigated as our first candidate a system in which the two phases contained two components A and B . The A – A and the B – B interactions are the same WCA type soft sphere repulsion with identical parameters. This pairwise additive short-range interaction, $\phi(r)$, is defined in terms of the distance between two particles, r , as follows:

$$\phi(r) = 4 \left[\frac{1}{r^{12}} - \frac{1}{r^6} \right] + 1, r < r^{1/6}$$

$$= 0, \quad r \geq r^{1/6}.$$

Here we used the usual reduced units of computer simulations [distances made dimensionless by dividing by the molecule diameter σ , energies made dimensionless by dividing by the characteristic interaction energy ϵ , temperature made dimensionless by multiplying by k/ϵ where k is Boltzmann's constant, number densities made dimensionless by multiplying by σ^3 , strain rates made dimensionless by multiplying by $(m\sigma^2/\epsilon)^{1/2}$, and times made dimensionless by dividing by $(m\sigma^2/\epsilon)^{1/2}$].⁴

The WCA repulsion of the A – B interaction, however, was more repulsive because of a larger σ value. This choice was motivated by our qualitative understanding of the phase-separation process. In equilibrium the two components mix because the free energy of the mixture is smaller than the sum of the free energies of the pure components. We expect the energy term to be the important contribution. If the system is shearing the molecules are rotating. The dissipation is large if the A and B molecules form a relatively rigid and extended complex. This rotating complex can be conceptualized as an increase in density or in the size of the particles because of the exclusion of other particles from the approximate sphere of rotation. Therefore the impact of shear can be considered in a very rough approximation as the increase of particle volumes. The phase separation at the expense of A – B interaction energy would prevent this effective volume enlargement.

We made two approximations in the algorithm. First, we omitted the time-consuming heat capacity calculations and identified the temperatures of the subsystems with their kinetic temperature. This crude approximation becomes exact for our model if the size of the two phases are identical. This is the result of the identical A – A and B – B interactions and particle masses and the equimolar concentrations in the composite system. The more different the size of the two phases the less correct this assumption is. Second, we handled the insertion–deletion procedure as if the particles were hard spheres with some effective diameter. This way we could

TABLE I. Results for the type I fluid simulations (see the text for details).

System	Shear rate	Temp.	Pressure	Density A1	Density B1	Density A2	Density B2
0.55	0.0	1.30	3.30	0.275	0.275	0.275	0.275
	0.0	1.31	3.25	the two	phases	unified	
0.50	0.0	1.35	2.68	0.25	0.25	0.25	0.25
	0.0	1.37	2.58	0.12	0.38	0.38	0.12
	0.5	1.37	2.60	0.11	0.39	0.45	0.05
	1.0	1.36	2.58	0.10	0.39	0.44	0.07
	2.0	1.35	2.62	0.06	0.44	0.48	0.02
0.45	0.0	1.40	2.14	0.225	0.225	0.225	0.225
	0.0	1.43	2.02	0.13	0.32	0.43	0.03
	0.75	1.40	2.11	0.15	0.30	0.38	0.07
0.40	0.0	1.44	1.70	0.20	0.20	0.20	0.20
	0.5	1.45	1.71	0.13	0.27	0.27	0.13

avoid the invocation of the time-consuming phase space compression factor calculation. Both of these approximations distort our results but still provide some indication of the demixing properties of this system and the numerical feasibility of such calculations.

The mixing of the two components is determined by two competing effects. The mixing decreases the free volume accessible for particle motion because of the larger number of more repulsive $A-B$ interactions. This effect decreases the entropy of the system. On the other hand the mixing entropy increases. The relative size of these two contributions determines the equilibrium state of the system.

If we shear the system we introduce an additional factor into this competition. The shear changes the structure of the fluid which changes the entropy of both the pure and the mixed phases. Since we had no *a priori* estimate on this effect we can only hope that at certain state points the impact of the shear will produce more or less demixing relative to the equilibrium system.

At the start each subsystem contained 128 A and 128 B type of particles. We performed simulations at four different reduced densities 0.40, 0.45, 0.50, and 0.55. The reduced density values were obtained by reduction of the like-like interaction diameter, σ . There were two different $A-B$ σ values tried at these densities: 1.1 and 1.2. In the following we refer to the former case as type I fluid and to the latter as type II fluid. The internal energy was fixed for each case at the value of 2.50 per particle in reduced units. The A and B particles occupied different regions in the beginning of the simulations. At such low densities, however, we expected fast mixing in each subsystem. The reduced time step varied between 0.004 and 0.0005 depending on the shear rate. A fifth-order Gear algorithm integrated the equations of motion. The coupling of the temperatures and the pressures in the two phases were determined by the equations given in Sec. II. It was, however, the P_{yy} component of the pressure tensor which determined the mechanical balance of the two phases.

Particle interchange attempts were made after 1.0 time units. A value of a random number determined which type of

particle should be created in which of the two subsystems. (First, a check was made whether the other subsystem contained this type of particle.) The program generated a random point in that subsystem and attempted an insertion at that point. If the insertion was unsuccessful the program attempted to insert the other type of particle into the same subsystem. If this was also unsuccessful the insertion of the other type of particle was tried in the original then, in the case of failure, in the other subsystem. If none of these four attempts were successful the program continued to run for 1.0 time units again. As we alluded to earlier, the acceptance criterion was based on an effective size of the two type of particles. For the $A-A$ and $B-B$ interactions, this was 1.06, while for the $A-B$ interaction the values were 1.166 and 1.272. These were the forbidden overlap distances. If the insertion succeeded the same type of particle was chosen at random and removed from the other subsystem. This determined the velocity of the inserted particle as we described earlier. (It should be noted that at high shear rates the large incremented streaming velocities were much less tolerant with the random peculiar velocity of the inserted particle. A small time step was necessary to prevent the divergence of the integrator.)

The simulations started in equilibrium. Each run was continued until the properties of the system settled around average values. After this we introduced the shear rate of 0.1 and continued the run again until the system properties ceased to change systematically. The 0.1 increment in the shear rate was applied until 0.5, then the increment became 0.25. The studied densities were chosen by several pilot runs. For higher densities the expected increase in the excluded volume effect caused by mixing was found to be overwhelming, resulting in complete phase separation in equilibrium without a chance to mix again under the impact of shear, while below 0.4 the system was so dilute that there was no inhibition against the perfect mixing. During the simulations we checked the homogeneity of the phases by monitoring several indicator numbers counting the type of neighbors around each particle.

The most important characteristics of the results are

TABLE II. Results for the type II fluid simulations (see the text for details).

System	Shear rate	Temp.	Pressure	Density A1	Density B1	Density A2	Density B2
0.55	0.0	1.29	3.32	0.275	0.275	0.275	0.275
	0.0	1.38	2.73	0.02	0.53	0.54	0.01
0.50	0.0	1.32	2.78	0.25	0.25	0.25	0.25
	0.0	1.35	2.64	the two	phases	unified	
0.45	0.0	1.37	2.29	0.225	0.225	0.225	0.225
	0.0	1.39	2.38	0.19	0.25	0.26	0.20
	0.5	1.36	2.35	0.22	0.23	0.23	0.22
	1.0	1.35	2.42	0.21	0.24	0.24	0.21
	1.5	1.34	2.43	0.17	0.28	0.26	0.19
	2.0	1.33	2.45	0.15	0.29	0.26	0.19
0.40	0.0	1.41	1.83	0.20	0.20	0.20	0.20
	2.5	1.37	2.02	0.19	0.21	0.21	0.19

shown in Tables I and II for types I and II systems, respectively. We identified the different cases with their overall density. The pressure means the yy element of the pressure tensor. Tables I and II show only the most important averages of the runs. In most of the cases there are two sets of values given for equilibrium (shear rate=0). The first set characterizes the relaxed starting state of the system without particle interchange and pressure coupling. The second shows the final equilibrium state after the two subsystems reached both pressure and composition equilibrium. Since the sizes of the phases sometimes were quite different the number density sums do not equal exactly the overall density in the case of a single component. The average balance densities of the two phases could also differ slightly as a result of the different subsystem volumes.

As can be seen from Tables I and II the composition equilibrium changed the properties of the phases in equilibrium. This change was most pronounced in the case of the high density phases. For the type II system at $\rho=0.55$ the phase separation became practically complete. As a result of this the kinetic temperature increased considerably. Even more remarkable is the substantial decrease in the pressure. (The higher temperature at fixed internal energy and the smaller pressure means “more comfortable” arrangements for the particles.)

It is interesting to compare these findings with results for the type I fluid at the same density. Both the temperature increase and the pressure decrease are small. We could not report results for the different densities because one of the two subsystems practically disappeared. Unfortunately, this phenomenon is a general tendency in the simulations. The composite system can decrease its entropy by unifying the two simulation cells. This tendency is strong if the mixing in one or in both of the phases is imperfect and/or the difference in the fluctuating volumes becomes large. In these cases, removal of a particle from the smaller subsystem and placement into the bigger one is an entropy gain comparable to the real effects at such a small system size. The occurrence of this transition is often accidental: repetition of the same simulation with different initial conditions can lead to differ-

ent results. This artefact may be eliminated by using much larger system sizes. The comparison of the data indicates that in the case of type I the unified system represents only a local entropy maximum for the system.

A similar simulation cell unification occurred at $\rho=0.50$ for type II. It was this tendency which halted the simulations of type II and type I at $\rho=0.45$ although in the first case we could reach the high shear rate region. At the lowest density ($\rho=0.40$) we experienced perfect mixing in equilibrium. (Therefore, we do not show a second set of data for zero shear rate.) In the case of type II the strong tendency to mix did not seem to change in the studied shear rate region. This was different for the type I fluid but the latter simulation was not pursued far enough to decide how permanent the separation is.

Partial demixing was experienced in the middle of our studied density range. The shear seemed to influence the separation of the components. We show two figures to see the effect more clearly. In the case of type I fluid at $\rho=0.50$, the shear-free demixing is considerable (Fig. 1). It takes ~ 2500 time units to reach equilibrium. During this time the volumes of the phases oscillate around their starting values. The shear seems to enhance the separation of the components although the fluctuations are much larger. Some uncertainty comes from the different volume sizes. Our temperature balance calculation is exact only if the two volumes are equal as we mentioned earlier. Therefore we should view this result with caution. In the case of the type II fluid, the $\rho=0.45$ system partially demixes at equilibrium (Fig. 2). Since this demixing is not very large this is achieved after a very short time. Then the system preserves this state in the shear-free region. At low shear this demixing seems to be reversed. The mixing becomes almost complete. A further increase of the shear rate supports the demixing again. Unfortunately, the volumes are quite different in the nonequilibrium region which raises questions about the validity of the temperature equilibrium. It should be further noted that the increase of the shear rate is not linear with time. In general, we spend more time at lower shear rates to detect small

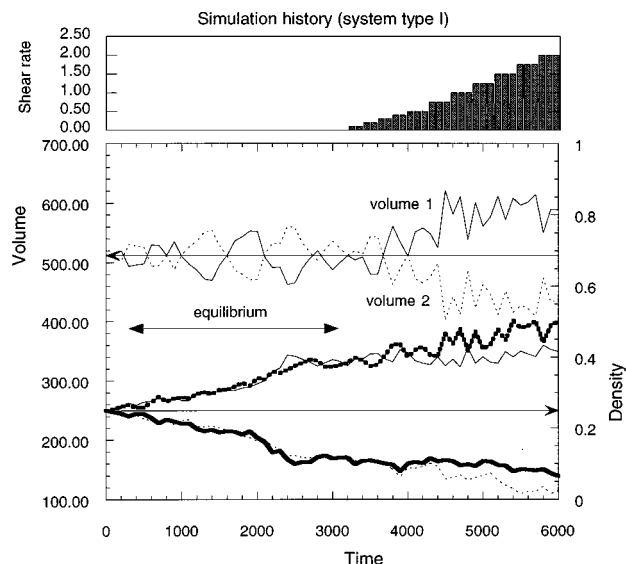


FIG. 1. Simulation history of our model system type I at the density of 0.50. (See the text for further details.) On the top of the graph the imposed shear rate as a function of time is shown. Below the volumes and the densities of the coexisting phases are depicted. Snapshots of the systems were taken at every 100th time unit. The average (or starting volume) and the average or starting densities are indicated by straight horizontal arrows. The symmetric appearance of the volume curves is the result of the total volume constraint. The densities indicated with one type of line belong to the volume indicated with the same type of line (solid or dashed). The thick lines refer to component A.

changes than at high shear rates where the impact of the external field is more pronounced.

Our overall conclusion is that in our model it is the competition between the entropy decrease coming from the larger excluded volumes and the increase from the mixing entropy which are the important factors. From the limited results obtained thus far, the influence of shear on this sys-

tem does not appear to be strong enough to warrant further exploration of this model, either with larger systems or a more precise version of the algorithm.

To test the accuracy and feasibility of our more rigorous approach will require a more realistic model system. Unfortunately, the experimental systems in which this phenomenon are observed⁵ are far too complex for direct simulation. It is also probable that the thermodynamic driving forces of the real phase transitions are quite subtle and thus difficult to detect in small simulated model systems. Therefore we did not attempt to capture a phase separation in shearing model systems with the more rigorous algorithm this time. However, we comment on numerical properties of the proposed method. These comments are conclusions of earlier calculations and several pilot runs with the more rigorous algorithm.

The increase of the shear rate can be done continuously⁸ or in a stepwise manner. We believe that the latter is more suitable because we can extend our run at the same shear rate value if the averages are not accurate enough. For simple liquids the size of the shear steps can vary between 0.01 and 0.1 in reduced units depending on the temperature and the density of the system. (The upper limit is applicable at low densities and high temperatures.) The length of each step should be at least several hundred thousand time steps if the desired accuracy of the heat capacities and phase space compression factors is better than several percent. These properties in equilibrium are closely related to fluctuations. The numerical estimation of a fluctuation amplitude, however, requires at least an order of magnitude longer calculation than the mean value of the same quantity at comparable accuracy.³²

A major difference between the equilibrium GEMC technique and this algorithm is that in the former all the properties of the system evolve stochastically toward their equilibrium value. The calculation of the phase space compression factor, however, requires long-run averaging. The local extremum of this average defines the true state of the system. This means that the particle insertion trials do not fail instantly (it does not really matter how we put the new particle in) but after several ten or hundred thousand time steps when we should return to the previous state of the system. In the case of the heat flow one has to do everything twice because of the application of the auxiliary phases. These parts are reasonably demanding even with present computer capacities.

V. CONCLUSIONS

We investigated the possibilities of deriving an algorithm for atomistic simulation of phase-coexistence problems in NESS systems. In particular, we studied the case of planar Couette flow because of its importance in rheology. Encouraged by the success of the GEMC method we adopted an analogous approach to NESS systems.

First, we derived an equilibrium molecular dynamics version of the GEMC technique. This MD algorithm handles the mechanical and temperature balances in a deterministic fashion but the chemical equilibrium is reached by a stochas-

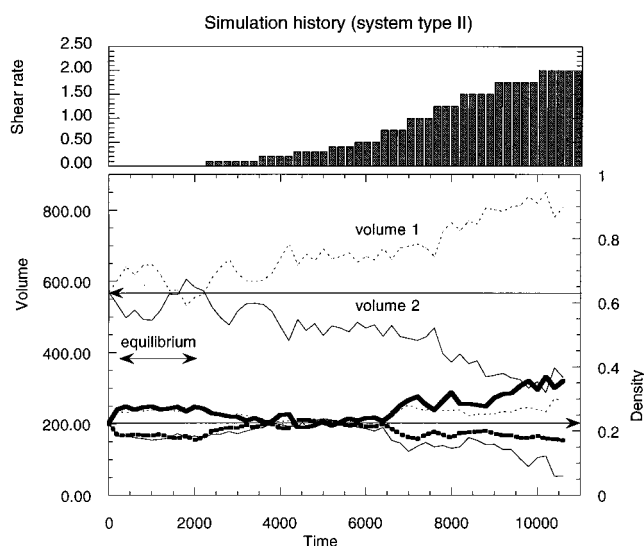


FIG. 2. The same as in Fig. 1 for system type II at the density of 0.45.

tic supplement assuming the ergodicity of the dynamical system. A further peculiarity of the equilibrium MD code is that the composite system is a member of the microcanonical ensemble and not the usual canonical. The fixed total energy still requires temperature balance between the two parts of the system but—for the sake of computational simplicity—this is achieved via a differential feedback scheme, which keeps the two temperatures strictly identical at every instant. Since the pressure equilibrium within the total volume constraint is solved by an integral feedback, the total volume is a more stable quantity than the total energy in the course of the simulation. Two technical problems contribute to the imperfection of this algorithm: one is the temperature error introduced by the particle exchange; the other is the small error in the trajectory integration after the particle exchange procedure by a non-self-starting integrator. However, none of these errors is principal in character and both of them can be overcome at some extra cost of programming and running time. Thus, the equilibrium MD version for multicomponent phase equilibrium is a reliable computational tool.

We might call the generalization of the equilibrium GEMD the GENEMD method in which the equations of motion are supplemented with the shearing terms as in the SLLOD equations. The GENEMD equations are identical to the GEMD equations in the case of the pressure. The only difference is that the anisotropy of the NESS system should be taken into account. Pressure balance should be established only in that direction which is perpendicular to the hypothetical interface. The volume changes can then be coupled to the pressure balance either in this direction only or in all three directions.

In the case of the thermal equilibrium, the two algorithms differ by the introduction of the heat capacity into the GENEMD version. However, a more important difference is that while the GEMD calculation can start at the particular E, V, N values of interest, the GENEMD calculation always should start from $\gamma=0$ whatever the target shear rate value might be. The calculation should then quasistatically move to the final shear rate value. This requirement, together with the unusual fixed total energy boundary condition, is the result of the fact that we do not know the value of the thermodynamic temperature which governs the thermal balance between the two coexisting phases.

It seems that this inconvenient coupling to the equilibrium state is the only way to circumvent the problem of unknown NESS thermodynamics. The same approach was used to calculate the entropy of NESS systems from the excess work. This excess work expression was shown to be equivalent with the minimum phase space compression principle. We utilized this principle for the chemical balance calculation because to our best knowledge there is no other way to do this. The generalization of the much simpler Widom method is approximate even for a NESS system of hard particles.

In principle the EB extremum property could be used for all three balance equations. However, this is inadvisable for both theoretical and computational reasons. First, the global validity of the EB extremum property is tied to the process

which measures the excess work. According to this, the maximum value of the entropy and the phase space compressibility is experienced relative to nearby states with the same E, V, N , and $\gamma(t)$ provided that in all the previous instants the transition followed the optimal, highest entropy path. Thus, the principle is not robust enough to test states far from this optimal path. We believe that, for a large enough system, an exchange of a single particle does not remove our system far from this optimal path. Clearly, the fulfillment of this requirement would be much more tenuous if we varied the pressure and the temperature as well.

Second, varying all the three variables would increase dramatically the number of possible states relative to the case when only the particle number is varied and tested. In our recommended scheme the pressure would assume the proper value automatically. As for the temperature balance it requires roughly the same computational effort as the calculation of the accurate phase space compressibility value. The two auxiliary systems double the cost of computation but the use of the EB principle requires twice as many test runs relative to the case when only the particle interchange is governed by the EB principle. The formulation of the heat balance is exact, while the EB principle is exact at least in the linear regime.

One might question the utility of our approach. It is based partly on principles rigorously unproved and is extremely time consuming. A brute force approach in which a large system in a NESS is simulated with the hope of undergoing phase separation might seem much simpler and rewarding. However, our experience shows that in strongly shearing systems the mixing of the two components becomes very slow compared to the equilibrium case. It is very easy to stay in a metastable state away from the correct property balance. For large molecules like polymers this metastable character together with the interference of the small system size can make such a realistic calculation prohibitively time consuming.

We performed several approximate calculations on a simple model system. The calculations provided some interesting results but also showed the limitations of the model. One would expect to see more pronounced effects of shear in systems containing elongated molecules in which the nature of molecule–molecule interaction differs considerably between isotropic state of the molecules at equilibrium and shear-aligned molecules in the presence of shear. Our present efforts are focused in this direction.

ACKNOWLEDGMENTS

P.T.C. gratefully acknowledges partial support of this research by the National Science Foundation through Grant No. CTS-9101326 and by Lockheed–Martin Energy Systems at Oak Ridge National Laboratory through the Distinguished Scientist program.

¹ A. Z. Panagiotopoulos, *Mol. Phys.* **61**, 813 (1987).

² *Computer Simulations in Chemical Physics*, edited by M. P. Allen and D. J. Tildesley, NATO ASI Series Vol. 397 (Kluwer, Dordrecht, 1993).

- ³D. J. Evans and G. P. Morriss, *Statistical Mechanics of Nonequilibrium Liquids* (Academic, New York, 1990).
- ⁴M. P. Allen and D. J. Tildesley, *Computer Simulation of Liquids* (Clarendon, Oxford, 1987).
- ⁵See, for example, R. Horst and B. A. Wolf, *Rheol. Acta* **33**, 99 (1994); B. A. Wolf, in *Rheological Modelling: Thermodynamical and Statistical Approaches*, edited by J. Casas-Vázquez and D. Jou (Springer, New York, 1991), pp. 194–214.
- ⁶D. Jou, J. Casas-Vázquez, and G. Lebon, *Rep. Prog. Phys.* **51**, 1105 (1988).
- ⁷D. J. Evans, *J. Stat. Phys.* **57**, 745 (1989).
- ⁸A. Baranyai and D. J. Evans, *Mol. Phys.* **74**, 353 (1991).
- ⁹A. Baranyai, D. J. Evans, and P. J. Davis, *Phys. Rev. A* **46**, 7593 (1992).
- ¹⁰J. Casa-Vázquez and D. Jou, *Phys. Rev. E* **49**, 1040 (1994).
- ¹¹A. Baranyai and P. T. Cummings, *Mol. Simul.* **17**, 21 (1996).
- ¹²B. L. Palmer and C. Lo, *J. Chem. Phys.* **101**, 10 899 (1994).
- ¹³D. J. Evans and A. Baranyai, *Mol. Phys.* **77**, 1209 (1992).
- ¹⁴J. M. Montanero, A. Santos, and V. Garzó, *J. Stat. Phys.* **81**, 989 (1995).
- ¹⁵I. Borzsák and A. Baranyai, *Phys. Rev. E* **52**, 3997 (1995).
- ¹⁶D. J. Evans and A. Baranyai, *Phys. Rev. Lett.* **67**, 2597 (1991).
- ¹⁷S. R. de Groot and P. Mazur, *Non-Equilibrium Thermodynamics* (Dover, New York, 1984).
- ¹⁸A. Santos, V. Garzó, and J. J. Brey, *Europhys. Lett.* **29**, 693 (1995).
- ¹⁹J. J. Brey, A. Santos, and V. Garzó, *Phys. Rev. Lett.* **70**, 2730 (1993).
- ²⁰S. Sarman, D. J. Evans, and A. Baranyai (unpublished).
- ²¹S. Sarman, *J. Chem. Phys.* **101**, 480 (1994).
- ²²W. G. Hoover and H. Posch, *Phys. Rev. E* **49**, 1913 (1994).
- ²³A. Baranyai (unpublished).
- ²⁴A. Z. Panagiotopoulos, N. Quirke, M. Stapleton, and D. J. Tildesley, *Mol. Phys.* **63**, 527 (1988).
- ²⁵S. Melchiona, G. Ciccotti, and B. L. Holian, *Mol. Phys.* **78**, 533 (1993).
- ²⁶R. Domínguez and D. Jou, *Phys. Rev. E* **51**, 158 (1995).
- ²⁷B. Widom, *J. Chem. Phys.* **39**, 2808 (1963).
- ²⁸J. P. Hansen and I. R. McDonald, *Theory of Simple Liquids* (Academic, New York, 1986).
- ²⁹I. Borzsák and A. Baranyai, *Chem. Phys. Lett.* **216**, 329 (1993).
- ³⁰W. Loose and S. Hess, *Physica A* **174**, 47 (1991).
- ³¹A. Baranyai and D. J. Evans, *Mol. Phys.* **72**, 229 (1991).
- ³²A. Baranyai and P. T. Cummings, *Phys. Rev. E* **52**, 2198 (1995).